B Physics at the Tevatron

Manfred Paulini
(Representing the CDF and DØ Collaboration)

Department of Physics, Carnegie Mellon University, Pittsburgh, PA 15213, USA

Received 20 Sept 2003

After a five year upgrade period, the Fermilab experiments CDF and DØ are taking high quality data in Run II of the Tevatron Collider. We report on the start-up of both detectors and present a selection of first B physics results from the Tevatron. We also compare different B hadron producers such as the $\Upsilon(4S)$ with the hadron collider environment and discuss general features of B physics at a hadron collider.

PACS: 13.20.He, 13.25.Ft, 13.25.Hw, 13.30.Eg, 13.85.Ni, 14.40.Lb, 14.40.Nd
Key words: charm particles; bottom particles; D mesons; B mesons; meson decay

1 Introduction

Traditionally, B physics has been the domain of e^+e^- machines operating on the $\Upsilon(4S)$ resonance or the Z^0 pole. But the UA 1 Collaboration has already shown that B physics is feasible at a hadron collider environment (see for example Ref. [1]). The first signal of fully reconstructed B mesons at a hadron collider has been published by the CDF Collaboration in 1992 [2]. CDF reconstructed a handful of $B^+ \to J/\psi K^+$ events in a data sample of 2.6 pb^{-1} taken during the Tevatron Run 0 at the end of the 1980's. Since then experimental techniques improved significantly, especially with the development of high precision silicon vertex detectors.

The CDF and DØ experiments can look back to an already successful B physics program during the 1992-1996 Run I data taking period (for a review of B physics results from, for example, CDF in Run I see Ref. [3]). Nowadays, B physics results from a hadron collider are fully competitive with the e^+e^- B factories. As discussed later in this review, with the operation of a hadronic track trigger, CDF reconstructs fully hadronic B decay modes without leptons in the final state. In many cases, the measurements performed at the Tevatron Collider are complementary to the B factories. For example, no B_S^0 mesons or baryons containing b quarks are produced on the $\Upsilon(4S)$ resonance.

2 Status of Tevatron Run II

2.1 The Upgraded Tevatron Accelerator

The Fermilab accelerator complex has undergone a major upgrade in preparation for Tevatron Run II. The centre-of-mass energy has been increased to 1.96 TeV as compared to 1.8 TeV during Run I. But most importantly, the Main Injector, a new 150 GeV proton storage ring, has replaced the Main Ring as injector of protons and anti-protons into the Tevatron. The Main Injector also provides higher

proton intensity onto the anti-proton production target, allowing for a luminosity goal of 1-2$\times 10^{32}$ cm^{-2}s^{-1}, representing a luminosity increase of more than an order of magnitude. The present bunch crossing time is 396 ns with a 36×36 $p\bar{p}$ bunch operation. An upgrade to a 132 ns bunch crossing time has been indefinitely postponed. The luminous region of the Tevatron beam has an RMS of $\sim$30 cm along the beamline (z-direction) with a transverse beamwidth of about 25-30 μm.

The initial Tevatron luminosity steadily increased from 2002 to 2003. By the summer of 2003, the peak luminosity reached by the Tevatron is $\sim 5 \cdot 10^{31}$ cm^{-2}s^{-1}. The total integrated luminosity delivered by the Tevatron to CDF and DØ by the time of this conference is $\sim$270 pb^{-1}. About 200 pb^{-1} were recorded to tape by each CDF and DØ. For comparison, the Run I data set comprised 110 pb^{-1}. However, most results shown in this review use about 70-110 pb^{-1} of data. The data taking efficiency of both collider experiments has reached about 80-95% on average.

2.2 CDF Detector Performance in Run II

The CDF detector improvements for Run II [4] were motivated by the shorter accelerator bunch spacing of up to 132 ns and the increase in luminosity by an order of magnitude. All front-end and trigger electronics has been significantly redesigned and replaced. A DAQ upgrade allows the operation of a pipelined trigger system. CDF's tracking system was completely renewed. It consists of a new Central Outer Tracker (COT) with 30 200 sense wires arranged in 96 layers combined into four axial and four stereo superlayers. It also provides dE/dx information for particle identification. The Run II silicon vertex detector consists of seven double sided layers and one single sided layer mounted on the beampipe covering a total radial area from 1.5-28 cm. The silicon vertex detector covers the full Tevatron luminous region and allows for standalone silicon tracking up to a pseudo-rapidity $|\eta|$ of 2. The forward calorimeters have been replaced by a new scintillator tile based plug calorimeter which gives good electron identification up to $|\eta| = 2$. The upgrades to the muon system almost double the central muon coverage and extend it up to $|\eta| \sim 1.5$.

The most important improvements for B physics in Run II are a Silicon Vertex Trigger (SVT) and a Time-of-Flight (ToF) system with a resolution of about 100 ps. The later employs 216 three-meter-long scintillator bars located between the outer radius of the COT and the superconducting solenoid. The Time-of-Flight system will be most beneficiary for the identification of kaons with a 2 σ-separation between π and K for $p < 1.6$ GeV/c. The SVT is discussed in more detail in Sec. 3.1.

2.3 The Upgraded DØ Detector

The DØ detector also went through a major upgrade before the beginning of Run II [5]. The inner tracking system was completely replaced and includes a new Silicon tracker surrounded by a Scintillating Fiber tracker, both of which are enclosed in a 2 Tesla solenoidal magnetic field. Pre-shower counters are located before the uranium/liquid-argon calorimeter to improve the electron and photon identifi-

cation. The already excellent muon system has been further improved by adding more shielding to reduce beam background.

The Run II DØ detector has excellent tracking and lepton acceptance. Tracks with pseudo-rapidity as large as 2.5-3.0 ($\theta \approx 10^\circ$) and transverse momentum p_T as low as 180 MeV/c can be reconstructed. The muon system can identify muons within $|\eta| < 2.0$. The minimum p_T of the reconstructed muons varies as a function of η. In most of the results presented, muons were required to have $p_T > 2$ GeV/c. Low momentum electron identification is currently limited to $p_T > 2$ GeV/c and $|\eta| < 1.1$. However, the DØ Collaboration is making serious attempts to improve both the momentum and η coverage.

A silicon based hardware trigger is being commissioned which will allow to trigger on long-lived particles, such as the daughters of charm and beauty hadrons. DØ expects to include this trigger in the online system by the end of 2003. DØ already applies impact parameter requirements in form of a software trigger at Level 3.

3 Features of B Physics at a Hadron Collider

In this section, we highlight some of the features of B physics at a hadron collider. We make an attempt to describe how B decays are studied at the Tevatron emphasizing some tools used to find B decay products in hadronic collisions.

We first compare different producers of B hadrons. Table 1 summarizes some of the important features of B physics experiments and the accelerators at which they operate. There are three main approaches to producing B hadrons. First, $e^+e^- \to \Upsilon(4S) \to B\bar{B}$ where the B factories dominate with the BaBar detector at SLAC and the Belle experiment at KEK. The pioneers of B physics at the $\Upsilon(4S)$ resonance were the CLEO experiment located at the CESR storage ring at Cornell and the ARGUS experiment at the DORIS storage ring at DESY. Second, $e^+e^- \to Z^0 \to b\bar{b}$ at the former LEP accelerator at CERN, as well as the SLD detector at the SLC Collider at SLAC. Finally, $p\bar{p} \to b\bar{b}X$ at the Tevatron, where the CDF and DØ detectors operate. The main motivation for studying B physics at a hadron collider is the large b quark production cross section $\sigma_b \sim 50$ μb within the central detector regions (see Table 1).

Figure 1(a) shows a typical B event at the $\Upsilon(4S)$ recorded with the ARGUS detector. At the $\Upsilon(4S)$ resonance, only $B^0\bar{B}^0$ or B^+B^- pairs are produced nearly at rest, resulting in a spherical event shape with an average charged particle multiplicity of about ten tracks. At the LEP or SLC accelerators, $b\bar{b}$ quark pairs are produced from the decay of the Z^0 boson where both quarks share half of the energy of the Z^0 resonance of 91.2 GeV. This results in two b jets being back-to-back. The average boost of B hadrons at the Z^0 resonance is $\beta\gamma \sim 6$.

Figure 1(b) represents a typical B event from CDF. No well-defined jet structure is visible; the average multiplicity is about 50 charged tracks including tracks from the "underlying event" particles. It might appear challenging to find the B decay products in this quite messy environment of a hadronic collision. One way to extract

Table 1. Comparison of important features of different experiments studying B physics.

	$e^+e^- \to \Upsilon(4S) \to B\bar{B}$	$e^+e^- \to Z^0 \to b\bar{b}$	$p\bar{p} \to b\bar{b}X$
Accelerator	PEP II, KEK, CESR	LEP, SLC	Tevatron
Detector	BaBar, Belle ARGUS, CLEO	ALEPH, DELPHI L3, OPAL, SLD	CDF, DØ
$\sigma(b\bar{b})$	$\sim$1 nb	$\sim$6 nb	$\sim$50 μb
$\sigma(b\bar{b}) : \sigma(had)$	0.26	0.22	$\sim$0.001
$B^0,\ B^+$	yes	yes	yes
$B_S^0,\ B_c^+,\ \Lambda_b^0$	no	yes	yes
Boost $<\beta\gamma>$	0.06	6	$\sim$1 - 4
$b\bar{b}$ production	both B at rest	$b\bar{b}$ back-to-back	$b\bar{b}$ not back-to-back
Multiple events	no	no	yes
Trigger	inclusive	inclusive	leptons, hadrons

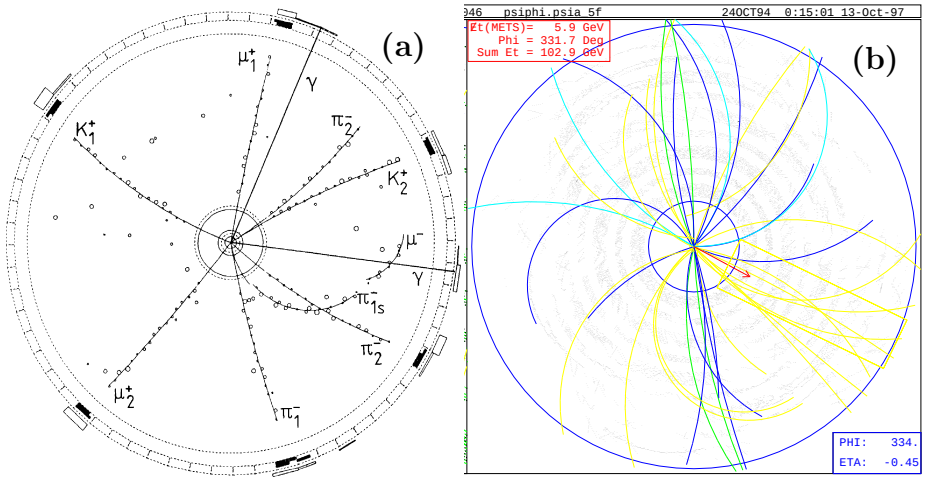

Fig. 1. (a) A typical B event at the $\Upsilon(4S)$ in the $r\,\varphi$ view from the ARGUS experiment. (b) A typical B event at the Tevatron recorded with the CDF detector.

B decays in a $p\bar{p}$ collision is to take advantage of the relatively long lifetime of B hadrons resulting in a B decay vertex which is clearly separated from the primary $p\bar{p}$ interaction vertex by hundreds of microns.

One important feature for B physics at a hadron collider is a good tracking capability which is usually achieved with a central tracking chamber. Together with a silicon detector assisting in tracking, an excellent track momentum resolution translates into an excellent invariant mass resolution, as illustrated in Fig. 2(a). Here, the dimuon invariant mass is displayed for muons from the Run I dimuon

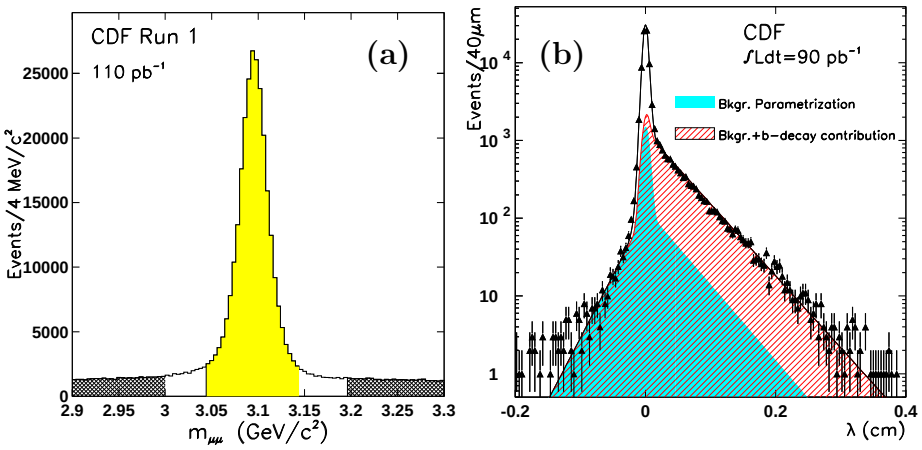

Fig. 2. (a) Invariant mass distribution of oppositely charged muon pairs from the CDF Run I dimuon trigger. (b) Decay length distribution of the J/ψ signal events.

trigger stream at CDF. A prominent J/ψ peak is visible on low background. The mass resolution of the J/ψ peak is about 16 MeV/c^2.

In addition to excellent tracking, superb vertexing is the other essential feature of successful B physics studies at a hadron collider. This is demonstrated in Fig. 2(b) where the two muons of the J/ψ signal candidates [light-shaded area in Fig. 2(a)] are vertexed using tracking information from the silicon detector. The two-dimensional distance between the primary $p\bar{p}$ interaction vertex and the reconstructed dimuon vertex is plotted. This distribution shows several features: a prominent peak at zero decay length results from prompt J/ψ candidates which are produced at the primary interaction vertex and constitute about 80% of all J/ψ candidates. The width of this peak reveals information about the vertexing resolution, which is on average 40-50 μm, for this sample. At positive decay lengths, J/ψ mesons from B hadron decays are described by an exponential slope. At a distance of about 100 μm from the primary interaction vertex, mainly J/ψ's from B decays remain. There is also a small exponential slope at negative decay lengths where the particle seems to decay before the point where it is produced. These events result from the combinatorial background underneath the J/ψ signal. This is indicated by events from the J/ψ sidebands [dark-shaded regions in Fig. 2(a)] which describe well the distribution at negative decay lengths as seen by the dark-shaded area in Fig. 2(b).

3.1 Triggering on B Decay Products

The total inelastic $p\bar{p}$ cross section at the Tevatron is about three orders of magnitude larger than the b production cross section. The CDF and DØ trigger system is therefore the most important tool for finding B decay products. In addition, the cross section for b quark production is steeply falling. It drops by almost two

orders of magnitude between a b quark p_T of about 8 GeV/c and 25 GeV/c. To find B decay products in hadronic collisions, it is desirable to go as low as possible in the decay products transverse momentum, exploiting as much as possible of the steeply falling b cross section. Of course, the limiting factor is the bandwidth of the experiment's data acquisition system.

In Run I, all B physics triggers at CDF and DØ were based on leptons including single and dilepton triggers. In Run II, both experiments still exploit heavy flavour decays which have leptons in the final state. Identification of dimuon events down to very low momentum is possible, allowing for efficient $J/\psi \to \mu^+\mu^-$ triggers. As a consequence, both experiments are able to fully reconstruct B decay modes involving J/ψ's. Triggering on dielectrons to isolate $J/\psi \to e^+e^-$ decays is also possible, although at low momentum backgrounds become more problematic. CDF has implemented a $J/\psi \to e^+e^-$ trigger requiring each electron $p_T > 2$ GeV/c.

Both experiments also use inclusive lepton triggers designed to accept semileptonic $B \to \ell\nu_\ell X$ decays. DØ has an inclusive muon trigger with excellent acceptance, allowing them to accumulate very large samples of semileptonic decays. The CDF semileptonic triggers require an additional displaced track associated with the lepton, providing cleaner samples with smaller yields.

New to the CDF detector is the ability to select events based upon track impact parameter. The Silicon Vertex Trigger gives CDF access to purely hadronic B decays and makes CDF's B physics program fully competitive with the one at the e^+e^- B factories. The hadronic track trigger is the first of its kind operating successfully at a hadron collider. It works as follows: With a fast track trigger at Level 1, CDF finds track pairs in the COT with $p_T > 1.5$ GeV/c. At Level 2, these tracks are linked into the silicon vertex detector and cuts on the track impact parameter (e.g. $d > 100$ μm) are applied. The SVT track impact parameter resolution is about 50 μm including a 33 μm contribution from the transverse beam spreading. The original motivation for CDF's hadronic track trigger was to select $B^0 \to \pi\pi$ decays to be used for CP violation studies.

4 Selected B Physics Results from the Tevatron

With the different B trigger strategies above, the Collider experiments are able to trigger and reconstruct large samples of heavy flavour hadrons. To give an idea about the sample sizes available for heavy flavour analyses, the approximate yield for $D^0 \to K^-\pi^+$ is ~ 6000 events per pb^{-1}, for $B^- \to D^0\pi^-$ it is ~ 16 events, for $J/\psi \to \mu^+\mu^-$ it is ~ 7000 events, for $B^- \to J/\psi K^-$ it is ~ 11 events or for $B \to D\ell\nu$ it is ~ 400 events per pb^{-1} at the Tevatron. In the following we discuss some selected B physics results from CDF and DØ.

4.1 B Hadron Masses and Lifetimes

Measurements of B hadron masses and lifetimes are basic calibration measures to demonstrate the understanding of heavy flavour reconstruction. For example, CDF uses exclusive B decay modes into J/ψ mesons for precision measurements of

Table 2. Summary of B hadron mass and lifetime measurements from CDF and DØ.

Mode	Mass (CDF) [MeV/c^2]	Lifetime (CDF) [ps]	Lifetime (DØ) [ps]
$B^0 \to J/\psi K^{*0}$	$5280.30 \pm 0.92 \pm 0.96$	$1.51 \pm 0.06 \pm 0.02$	$1.51 \pm 0.18 \pm 0.20$
$B^+ \to J/\psi K^+$	$5279.32 \pm 0.68 \pm 0.94$	$1.63 \pm 0.05 \pm 0.04$	$1.65 \pm 0.08^{+0.09}_{-0.12}$
$B_S^0 \to J/\psi\phi$	$5365.50 \pm 1.29 \pm 0.94$	$1.33 \pm 0.14 \pm 0.02$	$1.19 \pm 0.18 \pm 0.14$
$\Lambda_b \to J/\psi\Lambda$	$5620.4 \pm 1.6 \pm 1.2$	$1.25 \pm 0.26 \pm 0.10$	–

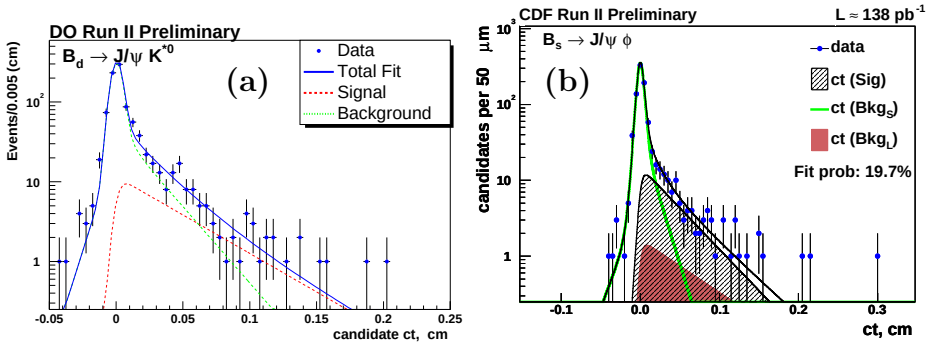

Fig. 3. Examples of proper decay length distribution for (a) $B^0 \to J/\psi K^{*0}$ at DØ and (b) $B_S^0 \to J/\psi\phi$ at CDF.

B hadron masses reconstructing the decay modes $B^0 \to J/\psi K^{*0}$, $B^+ \to J/\psi K^+$, $B_S^0 \to J/\psi\phi$ and $\Lambda_b \to J/\psi\Lambda$. These modes combine good signal statistics with little background. The results of the mass measurements are summarized in Table 2.

The proper time of a B decay is determined from the distance between the primary vertex of the $p\bar{p}$ collision and the B meson decay vertex measured in the plane transverse to the beam axis: $L_{xy}^B = (\vec{x}_B - \vec{x}_{prim}) \cdot \vec{p}_T/|\vec{p}_T|$, where $\vec{p}_T$ is the measured transverse momentum vector. At DØ, the primary vertex is reconstructed individually for each event. The typical resolution of L_{xy}^B is 40 μm. CDF uses the run-averaged beam position whose contribution to the L_{xy}^B uncertainty is $\sim$30 μm.

In the case of fully reconstructed B hadron decays, the proper lifetime τ is obtained by $c\tau = L_{xy}^B \cdot M_B/p_T$, where M_B is the B hadron mass. In the case of inclusive decays where the B hadron is not fully reconstructed, a boost correction obtained from a Monte Carlo simulation is usually applied. Both experiments have measured the lifetimes of the B^+, B^0 and B_S^0 mesons from the decay channels $B^+ \to J/\psi K^+$, $B^0 \to J/\psi K^{*0}$ and $B_S^0 \to J/\psi\phi$, respectively. Examples of proper decay length distributions and fit results are shown in Figure 3 for the decay mode $J/\psi K^{*0}$ at DØ and $J/\psi\phi$ at CDF. The resulting lifetime measurements from CDF and DØ are summarized in Table 2 which also includes preliminary measurements of the $\Lambda_b \to J/\psi\Lambda$ mass and lifetime from CDF.

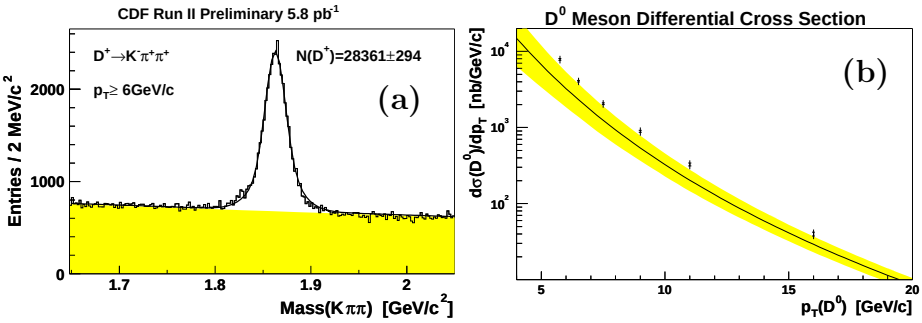

Fig. 4. (a) Yield for $D^+ \to K^-\pi^+\pi^+$ used in the charm cross section analysis. (b) The measured differential cross section for prompt $p\bar{p} \to D^0 X$, with $|y(D^0)| < 1$. The D^0 hadrons arising from B decays have been removed. The NLO calculation is from Ref. [7].

4.2 Prompt Charm Cross Section

Previously published measurements of the b production cross section at the Tevatron have consistently been higher than the Next-to-Leading-Order (NLO) QCD predictions. Although the level of discrepancy has been reduced with recent theoretical activity, it is not yet clear that the entire scope of the problem is understood. Both collider experiments will again measure the b and $b\bar{b}$ cross sections in Run II. To further shed light on this problem, CDF has recently presented a measurement of the charm production cross section [6]. Using the secondary vertex trigger, CDF has been able to reconstruct very large samples of charm decays. Figure 4(a) shows a fully reconstructed $D^+ \to K^-\pi^+\pi^+$ signal comprising almost 30k events using 5.8 pb^{-1} of data from the beginning of Run II.

Since the events are accepted based upon daughter tracks with large impact parameter, the sample of reconstructed charm decays contains charm from direct $c\bar{c}$ production as well as charm from B hadron decays $b \to c$. To extract the charm meson cross section, it is necessary to extract the fraction of D mesons that are coming from prompt charm production and remove the fraction from $b \to c$ decays. This is done by measuring the impact parameter of the charm meson. If it arises from direct $c\bar{c}$ production, the charm meson will have a small impact parameter pointing back to the primary $p\bar{p}$ interaction vertex. If the charm meson originates from B decays, it will typically not extrapolate back to the primary vertex. Using this technique, along with a sample of $K^0_S \to \pi^+\pi^-$ decays for calibration, CDF finds that 80-90% of the charm mesons originate from direct charm production. The shorter charm lifetime is more than compensated by the copious charm production in hadronic collisions.

The full analysis includes measurements of the differential cross sections for prompt D^0, D^+, D^{*+} and D^+_S meson production. The integrated cross section results for rapidity $|y| \leq 1$ are $\sigma(D^0, p_T \geq 5.5 \text{ GeV}/c) = (13.3 \pm 0.2 \pm 1.5)$ pb, $\sigma(D^{*+}, p_T \geq 6.0 \text{ GeV}/c) = (5.2 \pm 0.1 \pm 0.8)$ pb, $\sigma(D^+, p_T \geq 6.0 \text{ GeV}/c) = (4.3 \pm$

$0.1 \pm 0.7)$ pb and $\sigma(D_S^+, p_T \geq 8.0 \text{ GeV}/c) = (0.75 \pm 0.05 \pm 0.22)$ pb, respectively. Figure 4(b) shows the comparison between data and a NLO calculation for the differential D^0 cross section from Ref. [7]. The trend seen in this figure is the same for the other D species. The prediction seems to follow the measured cross section in shape, but the absolute cross section is low compared to the measured results. This difference in magnitude between the measured and predicted charm meson cross section is similar to the difference between data and theory seen in the B meson cross sections.

4.3 Hadronic Branching Ratios

4.3.1 Two-body Charmless B Decays

With the new SVT trigger, CDF has begun to measure B decays with non-leptonic final states. One set of modes of particular interest are rare charmless two-body decays as they are potential modes for CP violation measurements. Requiring the final state to consist of two charged hadrons ($B \to hh$), the following modes can be accessed: $B^0 \to \pi^+\pi^-$, $B^0 \to K^\pm\pi^\mp$, $B_S^0 \to K^\pm\pi^\mp$, and $B_S^0 \to K^+K^-$. The B^0 states are also reconstructed at the e^+e^- B factories, but the B_S^0 modes are exclusive to the Tevatron.

Although the branching fractions are small, the final state has two high-p_T tracks that are relatively efficient for the displaced-track trigger. Figure 5(a) shows the reconstructed signal where all tracks are assumed to have the pion mass. The luminosity used for this distribution is 190 pb^{-1}. A clear signal is seen but the width of the peak is significantly larger (41 MeV/c^2) than the intrinsic detector resolution. This is due to the overlap of the invariant mass distributions from the four decay modes. To extract the relative contributions, kinematic information and $\mathrm{d}E/\mathrm{d}x$ particle identification is used. The particle identification is calibrated from a large sample of $D^{*+} \to D^0\pi^+$ decays, with $D^0 \to K^-\pi^+$. The charge of the pion from the D^* uniquely identifies the kaon and pion, providing an excellent calibration sample for the $\mathrm{d}E/\mathrm{d}x$ system. Although the K-π separation is only $\sim 1.3\,\sigma$, this is sufficient to extract the various two-body B decay contributions.

Based on the derived fractions, CDF finds the ratio of branching ratios

$$\frac{\mathcal{B}(B^0 \to \pi^+\pi^-)}{\mathcal{B}(B^0 \to K^\pm\pi^\mp)} = 0.26 \pm 0.15 \pm 0.055,$$

and measures the CP asymmetry in the $B^0 \to K\pi$ decay mode to be

$$A_{CP} = \frac{N(\bar{B}^0 \to K^-\pi^+) - N(B^0 \to K^+\pi^-)}{N(\bar{B}^0 \to K^-\pi^+) + N(B^0 \to K^+\pi^-)} = 0.02 \pm 0.15 \pm 0.017.$$

This analysis includes the first observation of the $B_S^0 \to K^+K^-$ decay mode. Turning the observed yields into a ratio of branching ratios, CDF obtains

$$\frac{\mathcal{B}(B_S^0 \to K^+K^-)}{\mathcal{B}(B^0 \to \pi^+\pi^-)} = 2.71 \pm 0.73 \pm 0.35 \pm 0.81,$$

where the systematic uncertainty on f_s/f_d is separately included as the last error.

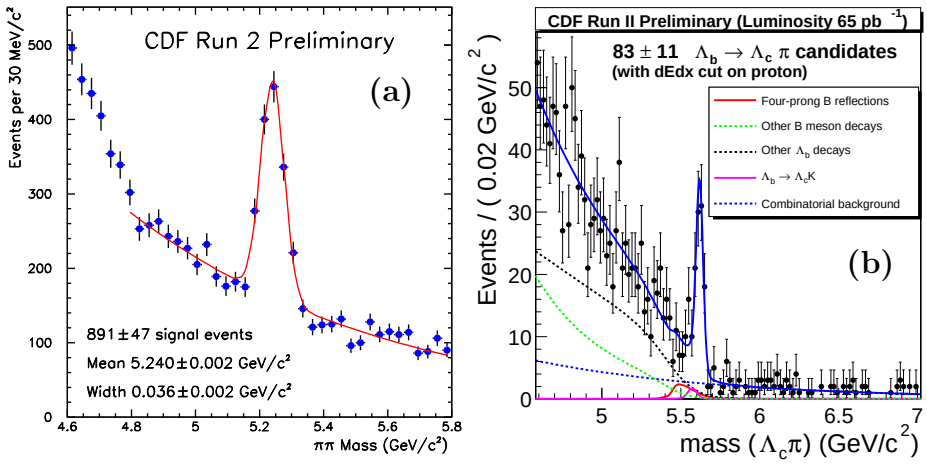

Fig. 5. (a) The reconstructed two-body $B \to hh$ ($h = \pi, K$) sample from CDF assuming M_π for both particles. (b) The CDF fully reconstructed $\Lambda_b \to \Lambda_c \pi$ with $\Lambda_c \to pK^-\pi^+$.

4.3.2 $\Lambda_b \to \Lambda_c \pi$ Branching Ratio

Using the SVT trigger, CDF has also measured purely hadronic b-baryon states. Figure 5(b) shows a clean signal of the decay $\Lambda_b \to \Lambda_c \pi^-$, with $\Lambda_c \to pK^-\pi^+$. The reconstructed invariant mass plot displays an interesting background structure, with almost no background above the Λ_b peak and a background that rises steeply going to lower mass. This structure is somewhat unique to baryon modes, which are the most massive weakly decaying B hadron states. Because the SVT trigger specifically selects long-lived states, most of the backgrounds are coming from other heavy flavour (b and c) decays. Since there are no weakly decaying B hadrons more massive than the Λ_b, there is very little background above the peak. On the other hand, going to masses below the peak, lighter B mesons begin to contribute. The background in this mode is growing at lower masses because there is more phase space for B^+, B^0, and B_S^0 decay modes to contribute.

To extract the number of signal events, $b\bar{b}$ Monte Carlo templates are used to account for the reflections seen in the signal window. The shapes of these templates are fixed by the simulation, but their normalization is allowed to float. The number of fitted signal events from this distribution is $96 \pm 13^{+6}_{-7}$. The primary result from this analysis is a measurement of the $\Lambda_b \to \Lambda_c \pi^-$ branching ratio relative to the kinematically similar $B^0 \to D^-\pi^+$ mode. Taking that ratio, along with the PDG [8] values for measured branching ratios and production fractions, CDF extracts $BR(\Lambda_b \to \Lambda_c \pi^-) = (6.5 \pm 1.1 \pm 0.9 \pm 2.3) \times 10^{-3}$, where the errors listed are statistical, systematic and the final uncertainty originates from the errors in the $B^0 \to D^-\pi^+$ branching ratio, the uncertainty on the ratio of f_{baryon}/f_d fragmentation fractions and in particular the $\Lambda_c \to pK\pi$ branching ratio.

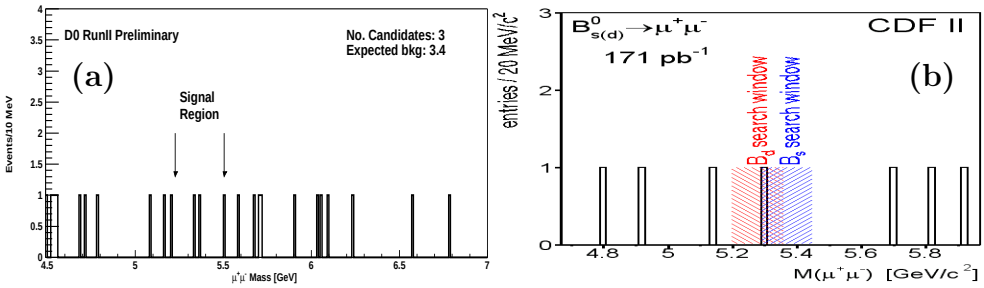

Fig. 6. Invariant dimuon mass distribution in the search for $B_S^0 \to \mu^+\mu^-$ from (a) DØ and (b) CDF.

4.4 Rare Decays

Flavour changing neutral currents (FCNC) are prohibited on tree-level in the Standard Model (SM). Contributions from sources beyond the SM might measurably enhance the low SM branching fractions of these rare decays. This explains the considerable theoretical interest in $B_S^0 \to \mu^+\mu^-$ [9]. In some models, non-SM contributions are large enough to allow an observation of this decay mode in Run II.

Experimentally there is considerable background of direct muon pairs in the spectrum of reconstructed muons. This is reduced by requiring the two muon tracks to form a displaced vertex and selecting candidates with a minimum transverse momentum of $p_T > 4.0$ GeV/c, in addition to the requirement that each muon is isolated. After applying these cuts in the DØ analysis, three B_S^0 candidates remain as shown in Figure 6(a). This is consistent with a background expectation of 3.4 events. Using the Feldman-Cousins method, DØ obtains a limit on the branching ratio of $BR(B_S^0 \to \mu^+\mu^-) < 1.6 \cdot 10^{-6}$ at the 90% confidence limit. This result is competitive with the CDF Run I limit.

Using data selected with the dimuon trigger, CDF has also searched for the flavour-changing neutral current decay $B_S^0 \to \mu^+\mu^-$. After applying optimized selection criteria, one event remained in the B_S^0 search window as shown in Fig. 6(b). This yields an improved upper limit on the branching fraction of 9.5×10^{-7} (1.2×10^{-6}) at the 90% (95%) confidence level. This is more than a factor of two improvement over the previous limit produced by CDF in Run I. In addition, an upper limit on the branching fraction of $B^0 \to \mu^+\mu^-$ is derived simultaneously yielding values of 2.5×10^{-7} and 3.1×10^{-7} at the 90% and 95% confidence levels, respectively.

Data selected with the displaced track trigger were used to improve the limit on the branching fraction of the FCNC decay $D^0 \to \mu^+\mu^-$. This search begins by reconstructing a clean sample of the kinematically similar $D^0 \to \pi^+\pi^-$ decays using a D^* tag, followed by muon identification to select $D^0 \to \mu^+\mu^-$ candidates. The $D^0 \to \pi^+\pi^-$ decays serve also as normalization mode. A new upper limit of 2.5×10^{-6} at the 90% confidence level is derived from zero candidates in the search window. It is almost a factor of two better than the previous best limit.

5 Conclusion

After a five year upgrade period, the CDF and DØ detectors are back in operation taking high quality data in Run II of the Fermilab Tevatron Collider with all subsystems functional. These include new tracking systems with new central tracking devices and silicon vertex detectors for both experiments as well as a hadronic track trigger for CDF. The understanding of both detectors is well advanced and first physics results have been presented. We also compared different B hadron producers such as the $\Upsilon(4S)$ with the hadron collider environment and discussed general features of B physics at a hadron collider.

We reported on the start-up of both Tevatron detectors and presented a selection of first B physics results from the Tevatron including B hadron masses and lifetimes, measurements of the prompt charm cross section, hadronic branching fractions and rare decays. The prospects for one of the "flagship" B physics measurements in Run II, the observation of B_S^0 flavour oscillations, is discussed in detail in a another contribution to these proceedings [10]. More information about various other B physics prospects at the Tevatron in Run II can be found in Ref. [11].

I like to thank the organizers of this stimulating meeting for an excellent conference and my colleagues from the CDF and DØ collaboration for their help in preparing this talk and the proceedings. This work was supported by the U.S. Department of Energy under Grant No. DE-FG02-91ER40682.

References

[1] N. Ellis and A. Kernan, Phys. Rept. **195** (1990) 23.

[2] F. Abe *et al.* [CDF Collaboration], Phys. Rev. Lett. **68** (1992) 3403.

[3] M. Paulini, Int. J. Mod. Phys. A **14** (1999) 2791 [hep-ex/9903002].

[4] R. Blair *et al.* [CDF-II Collaboration], *"The CDF-II detector: Technical design report,"* FERMILAB-PUB-96-390-E (1996).

[5] S. Abachi *et al.* [The D0 Collaboration], *"The D0 upgrade: The detector and its physics,"* FERMILAB-PUB-96-357-E (1996).

[6] D. Acosta *et al.* [CDF Collaboration], Phys. Rev. Lett. **91** (2003) 241804 [hep-ex/0307080].

[7] M. Cacciari and P. Nason, JHEP **0309** (2003) 006 [hep-ph/0306212].

[8] K. Hagiwara *et al.* [Particle Data Group Collaboration], Phys. Rev. D **66** (2002) 010001.

[9] A. Dedes, H. K. Dreiner and U. Nierste, Phys. Rev. Lett. **87** (2001) 251804 [hep-ph/0108037];
R. Arnowitt, B. Dutta, T. Kamon and M. Tanaka, Phys. Lett. B **538** (2002) 121 [hep-ph/0203069];
G. L. Kane, C. Kolda and J. E. Lennon [hep-ph/0310042].

[10] S. Menzemer; these proceedings (2003).

[11] K. Anikeev *et al.*, FERMILAB-PUB-01-197 (2001) [hep-ph/0201071].